Hindawi
Advances in Civil Engineering
Volume 2023, Article ID 4732353, 11 pages
https://doi.org/10.1155/2023/4732353

Research Article

Numerical Study on Optimization of Piled Raft Foundation on Stratified Soil under Static Load

Getasew Mare Yirsaw[1] and Argaw Asha Ashango[2]

[1]*Department of Civil Engineering, Injibara University, Injibara 6040, Ethiopia*
[2]*Department of Civil Engineering, Adama Science and Technology University, Adama 1888, Ethiopia*

Correspondence should be addressed to Argaw Asha Ashango; argaw.asha@astu.edu.et

Received 2 June 2023; Revised 8 August 2023; Accepted 9 October 2023; Published 30 October 2023

Academic Editor: Massimo Latour

Piled raft foundation (PRF) is a combination of pile and raft that provides adequate bearing capacity under the allowable settlement. This research aims to optimize the PRF design for a 48-story Commercial Bank headquarters building in Addis Ababa, Ethiopia, by conducting parametric study on various pile configuration using FLAC3D (Fast Lagrangian Analysis of Continua in three Dimensions) software. We analyzed 28 piled raft configurations and found that increasing the distance between piles increases the raft load sharing distribution by 11.5% while reducing settlement. Despite variations in pile length and diameter, a close load sharing between the pile and raft is accomplished at a separation of seven times the pile diameter (7D). The largest settlement decrease achieved was 9% for a 2-m pile diameter by doubling the pile length from 10 to 20 m, indicating that increasing pile length is ineffective for settlement reduction. We also proposed two new pile configurations that share load equally among pile and raft, and slightly increase total settlement below 10-cm limit. The results show that the first configuration exceeds differential settlement limit, but the second configuration reduces it by 95% and saves 40% of piles. This study provides a useful reference for designing PRF for high-rise buildings in similar soil conditions.

1. Introduction

In conventional foundation design, it was customary to consider first, the use of shallow foundations like strips, combined, or rafts. If it is not adequate, a deep foundation which is a fully piled foundation is used instead. The scarcity of land in urban areas, intention for future purposes, advancement in technology, to use as a landmark has boosted the construction of high-rise buildings in the hub of Addis Ababa. In shallow foundations, it is supposed that a load of the superstructure is transmitted to the underlying ground directly by the isolated footings. However, in deep foundations, especially pile foundations, the entire design load is supposed to be carried by the piles [1]. The concept of piled raft foundations (PRFs) in the design of pile group was adopted and described by several authors, including Katzenbach et al. [2], Mandolini et al. [3], Poulos and Bunce [4], Poulos [1, 4, 5], and Reul and Randolph [6] among many. Analysis of PRF is useful to assess the ultimate load capacity for a vertical and lateral load, maximum differential settlement, raft moments, and shears. The analysis method ranges from a simplified method involving hand calculations to a more rigorous methos that uses numerical methods [5–9].

Considerable research has been done to understand how PRFs respond to static loads using numerical [8–16] and experimental [17–20] methods. Even while the raft's significance as a load-bearing element is maintained by the traditional design, the experimental results show that the proportion of load carried by the raft is substantially higher than 20% [17–19] and can be further adjusted by widening the space between piles [2–4]. Reul and Randolph [6] have discovered installing piles in the center and using longer piles than a large number of piles has resulted in a decent change in settlement reduction. Sinha and Hanna [8] have conducted a numerical analysis to examine the effect of the key parameters governing the performance of PRF on homogenous soil during loading and, accordingly, the load shared by the piles and the raft. Their results show an increase of spacing beyond 6D leads rafts to carry the whole

load, they also discovered thinner rafts may lead to a nonuniform load to be shared by the pile.

Moayedi et al. [21] have studied an analytic investigation on the performance of floating piled rafts on compressible soil layers for controlling angular distortion. They found that the angular distortion is lower when floating piles of different lengths are used rather than uniform lengths. Ko et al. [22] proposed a 3D interactive analysis of superstructure and PRF at once. They found iterative and interactive analysis gave similar results of settlement and raft bending moment compared with finite element analysis. Bernardes et al. [10] studied the use of PRFs for settlement control in grain silos, by performing numerical analyses with instrumented structures, and from this they found out the geometric factor equals 0.09 as a proposed optimized solution to reduce differential and total settlements. More research on PRF under stratified soil is necessary to reduce expenses from the overconservative design method. This is done through a thorough parametric study under various pile numbers, lengths, diameters, spacing, and raft thickness.

Although a great deal of effort has been made to study the performance and response of PRF under static loads, most works focused on clayey soil and one soil type or layered soils modeled as equivalent homogenous soil [6, 22]. In addition, limited research is available on the optimization of piles through a parametric study of on layered soil. A lot of studies are focused either to reducing the settlement to the allowable limit, or to estimate the load sharing between pile and raft [10]. The main objective of this study is to provide an optimized piled raft configuration based on the result of a thorough parametric study without compromising the design benchmarks. Numerical method has been a firsthand tool to investigated the bearing behavior, and total and differential settlement of PRF by various experts [23]. FLAC3D numerical software is used to conduct a thorough parametric investigation on various pile number, length, diameter, spacing, and uniform raft thickness is done. Appropriate constitutive model was selected considering; ability to get the desired parameter, capability to handle 3D condition, and quality of the model to fit with the observed experimental test [24]. Result of the numerical solution heavily depends on reproducing the true in-situ stress condition through following the in-situ construction sequence of PRF. The selection of piled raft geometry is taken from recommendation of EBCS-7 (1995) for bored piles and common practices [2, 8, 25]. Significant piled raft geometric components are pinpointed, and an optimized layout of PRF is proposed.

2. Materials and Methods

This methodology is driven and formalized from the kinds of literature reviewed and it is mainly plotted into the following generalized procedures as shown in Figure 1.

2.1. Description of the Study Area and Geologic Conditions of the Site. The commercial bank of Ethiopia (CBE) building site is located around Biherawi along Ras Dest Damtew Road with an area of 527 square km and elevation of 209 m in Cherkos Sub city, Addis Ababa. The CBE headquarter has

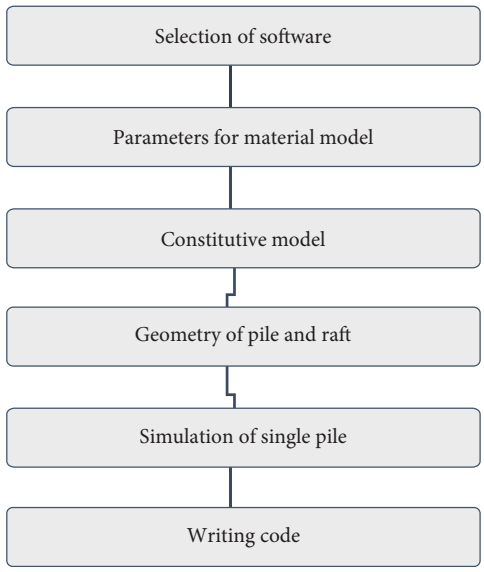

Figure 1: Procedure for the numerical study.

Figure 2: Commercial bank headquarter building.

three buildings namely: tallest building and two 5-story buildings. The CBE headquarters skyscraper (tallest building) has 48 stories and 20-m-deep underground parking lot (four basement levels) and two 5-story podiums as depicted in Figure 2. The subsurface exploration discovered that the underlying geologic condition is highly stratified consisting of silty clay to hard basaltic rock. Loose variegated, poorly graded fill material was encountered above 6.5 m while the second layer has 15.5-m thickness with a relatively dense silty clay soil. The third layer is a medium weathered basaltic rock of 6-m thickness underlaid by 9-m thick dense silty clay soil with a mixture of scoriaceous basaltic rock. The last layer is located at 47 m below the natural ground level having strong basaltic rock increasing in stiffness with depth. The groundwater table was encountered at an average depth of 6.5 m below the ground level in the majority of the boreholes. Table 1 depicts parameters that are used to model the geology conditions at the site for numerical investigation.

3. Mathematical Model and Constitutive Model

The equation of motion by applying a continuum form of momentum yields Cauchy's equations of motion (Equation (1)).

Table 1: Soil parameters for base model.

Layer	υ (-)	E (MPa)	G (MPa)	K (MPa)	c (kPa)	ϕ (°)	ρ (kg m^{-3})	SPT
1	0.32	16.45	6.23	137.10	25.3	19.5	1524	28
2	0.35	34.94	12.94	349.42	27	21.3	1743	38.5
3	0.3	45.99	17.69	344.89	28	37.4	2359	43
4	0.25	1027	410.80	684.67	5000	40	2626	49
5	0.32	265.5	100.57	245.83	25	35	1871	36
6	0.25	1680	672.00	1,120.00	5000	45	2886.7	>50
Conc. C-35	0.15	31,368	13,638.26	14,937.14	–	–	2500	

υ = Poisson's ratio; E = young's modulus; G = shear modulus; K = bulk moduli; c = cohesion; ϕ = internal angle of friction; ρ = density of material; SPT = the number of standard penetration test for 30 cm; Conc. C-35 = a concrete used for both pile and raft.

This law governs the motion of elementary volume when subject by a force. ρ is the mass-per-unit volume of the medium, b is the body force per unit mass, dv/dt is the material derivative of the velocity, and $\sigma_{ij,j}$ is the stress tensor. Hence, this equation governs the motion of any medium under both static and dynamic forces [26] as follows:

$$\sigma_{ij,j} + \rho b_i = \rho \frac{dv_i}{dt}. \tag{1}$$

For static analysis of continuum, the equation of motion will be changed into Equation (2) as follows:

$$\sigma_{ij,j} + \rho b_i = 0. \tag{2}$$

A geologic material especially, soil is a complicated material that behaves nonlinearly and often shows anisotropic and time-dependent behavior when subjected to different loading types [27, 28]. Lade [24] pointed out criteria for selecting an appropriate constitutive model. These are the ability to get the desired parameter, the ability to handle 3D conditions, the quality of the model to fit with the observed experimental test and simplicity. Based on these criterions an elastic perfectly plastic Mohr–Coulomb model has selected to model the soil and an elastic model was selected to model hard rock and concrete. This model was used by different studies; Sinha and Hanna [8], Giannopoulos [9], Alhassani and Aljorany [12], and it is found effective.

3.1. Simulation of Single Pile Capacity. The pile capacity for the axial load can be approximately calculated using an analysis method driven from empirical formulas which depend on the soil type, the method of installation, the pile type, and others. Considering this, it is possible to determine the pile capacity approximately and subsequent simulation on FLAC3D V6 is possible. The skin friction involves transferring force through the rough surface of the pile in cohesionless soil and the cohesion between the pile and surrounding soil in cohesive soil. Equation (3) is used for clay and sandy soils under effective and total stress analysis [29].

$$Q_S = \sum_{1}^{n} A_s f_s, \tag{3}$$

where A_s = effective pile surface area on which f_s acts; f_s is the shear stress capacity along the pile shaft which depends mainly on the unconfined shear strength of the soil (f_s) for fine-grained soils. The shear stress f_s of bored and cast in place pile on weathered and coarse-grained soil is calculated using the correlation with standard penetration test in Equation (4) [30].

$$f_s = a + bN \leq 200\,\text{kPa}, \tag{4}$$

where $a = 20$; $b = 2\,N$; and N = SPT—number of blows. Since the soil is highly weathered rock; $f_s = 200$ kPa. The total skin resistance of the pile $Q_s = A_s f_s = 6,280$ kN. The tip resistance of this pile is calculated from the unconfined compressive strength of the bedrock. Goodman and Kulhawy [30] in the 1980s proposed Equation (5) for bearing capacity of a pile standing on a rock. Where $N_\phi = \tan^2(45 + \phi'/2) = 4.11$ and $q_{u(\text{deisgn})} = 37.8/5 = 7.56$ MPa are the design unconfined compressive strength of the rock and it is laboratory result divided by a factor of five, $\phi' = 37.4°$ is drained angle of internal friction of rock. Using the Goodman and Kulhawy [30] formula, the end resistance of pile (Q_b) is 30.3 MN. Using a factor of five to account for discontinuity in the rock mass the allowable end resistance is 6.06 MN. The total load capacity using a factor of three for the skin resistance is 8.15 MN [11, 31].

$$q_p = q_{u(\text{design})}\left(N_\phi + 1\right). \tag{5}$$

The interface between the pile, the surrounding soil, and the base rock has both cohesive and frictional nature. These properties are called the shear and normal coupling spring. The shear coupling spring consists of the shear spring stiffness (Ks), shear direction friction angle ($\varnothing' s = tan\text{-}1((2/3) \times tan\varnothing')$), and shear direction cohesion ($c's = 2/3c'$). The normal spring stiffness (Kn), normal direction friction angle ($\varnothing' n = tan\text{-}1[(2/3) \times tan\varnothing']$), normal direction cohesion ($c'n = 0.9c'$) are used to model the interface in the direction to normal to the pile periphery. The above interface parameters are determined through a parametric study (trial and error) until the required bearing capacity and allowable

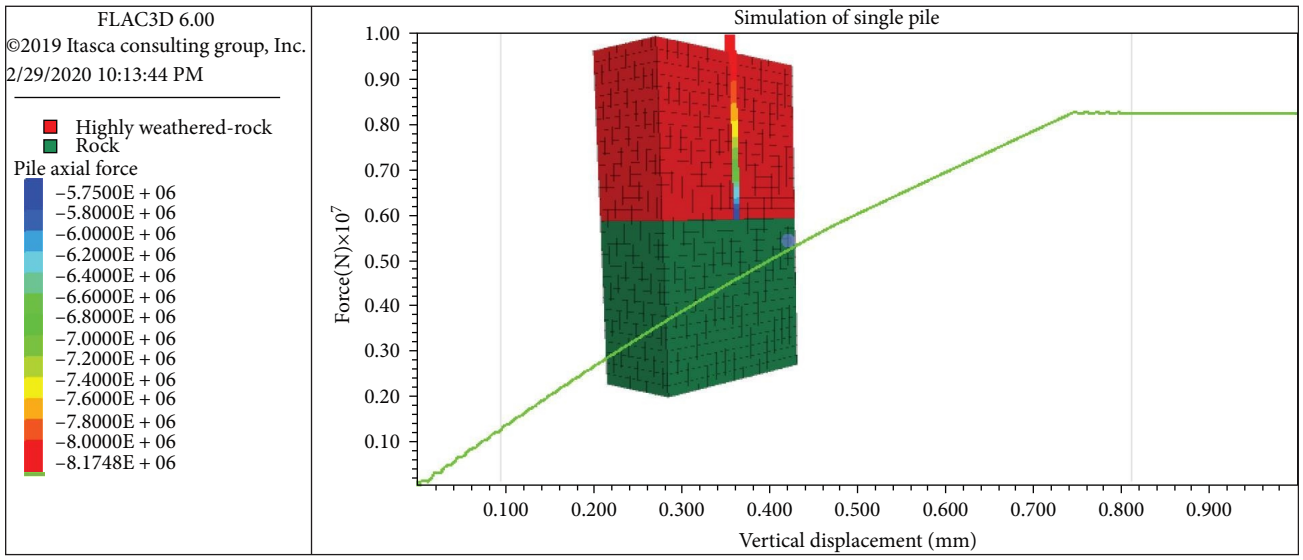

Figure 3: The plot of force versus displacement for a single pile having end and frictional resistance.

settlement are achieved. Different study indicates that the interface parameters for initial simulation can be approximated instead of initial assumptions [32–35]. While the shear and normal spring stiffness (*Kn*, *Ks*) are approximated and shown in Equation (6)

$$K_s = K_n = (10 - 100) \times \left[\frac{K + \frac{4}{6}G}{\Delta Z_{\min}}\right]. \quad (6)$$

Interface parameters are determined through a parametric study (trial and error) until the required bearing capacity and allowable settlement is achieved. The variation of the above interface parameters will be varied until 1% and 10% of the pile diameter is mobilized for shaft and end resistance, respectively [34]. Considering the above criteria, the simulation result of single pile for 10-mm pile diameter is shown in Figure 3. The simulation result shows that the settlement increase with increase in load up to 0.72 mm then constant.

3.2. Sensitivity Analysis and Grid Independency Test. Sensitivity analysis is a useful parametric study to obtain the optimum boundary size, mesh size, and mesh quality [28]. The finite number of mesh and distance of boundary from the piled raft will influence the results. To investigate the influence of the above-listed condition on a settlement, bearing capacity, and load sharing of PRF a sensitivity analysis was conducted.

Considering the above conditions four different boundary sizes and mesh quality are investigated and their influence is studied in detail. The settlement at the center and edge, an axial load of the pile at the center and edge and lateral load at the center and edge were investigated. Depending on the result a boundary size of $50 \times 50 \times 60$ m (length × width × depth) and 142,800 number of zones was selected for further parametric study under vertical loading (Tables 2 and 3). This selection has a very good aspect ratio (>0.7), volume ratio (>0.9), and orthogonality (>0.7). Therefore, further parametric study is valid and results are not highly influenced by the selected mesh fineness, mesh quality, and boundary size (Figure 4).

3.3. Analysis Procedure via FLAC3D. In this finite difference analysis, the soil and rock are modeled as eight nodded brick elements including wedge-shaped meshes. The long-term behavior of the geologic condition was taken since the water was pumped out before installation of pile, higher static vertical load results in the expulsion of water from the pores of the soil medium. The result of the numerical solution depends on the reproducing true in-situ stress condition and general procedure for the construction of PRF. Figure 5 shows the procedure used for the simulation of all 27 PRFs under vertical static load.

3.4. Parameters of PRF. In the parametric study square, both unpiled rafts and piled rafts with plan length of $B = 39$ m had considered. Each three unique pile spacing, length, and diameters were considered with a combination to 27 different piled raft arrangements. The geometric variables of the PRF that undergone numerical investigation is summarized as shown in Table 4. The headquarters uniform pile thickness of 3 m subjected to a distributed load of 926.7 kPa was taken.

3.5. Validation of Numerical Studies. The American Society of Civil Engineers (ASCE) Technical Committee-18 (TC-18) report by Poulos [1], has been used in this numerical study for the validation purposes. The results of the simulated model through different rigorous and simplified method have a settlement of around 50 mm. While in FLAC3D V6 the piled raft has a settlement of around 59 mm which is 85% accurate (Figure 6).

4. Results and Discussion

The main aim of this pile raft configuration is an investigation of the response of different pile geometric positioning under the raft. The magnitude of the superstructure load is

Table 2: Influence of boundary size on the PRF foundation.

Boundary size ($X \times Y \times Z$) m	No. of zones	Settlement (mm)		Axial load (MN)		y-Lateral load (MN)		z-Lateral load (MN)	
		Center	Edge	Center	Edge	Center	Edge	Center	Edge
$40 \times 40 \times 60$	13,606	39	29	8	19	−0.2	−0.8	0.2	0.84
$45 \times 45 \times 60$	21,756	40	29	8	18.7	−0.2	−0.8	0.2	0.82
$50 \times 50 \times 60$	24,864	41	30	8	18.6	−0.2	−0.8	0.2	0.78
$60 \times 60 \times 60$	29,008	43	30.5	8.2	18.4	−0.2	−0.8	0.2	0.78

Table 3: Influence of grid number on the PRF analysis.

Trial	No. of zones	Settlement (mm)		Axial load (MN)		Time taken (hr)
		Center	Edge	Center	Edge	
1	17,234	33	22	11	21.3	0.5
2	24,864	41	30	8	18.6	1
3	142,800	46	40	7.2	15	4.5
4	306,516	48	45	6.5	13.4	13.5

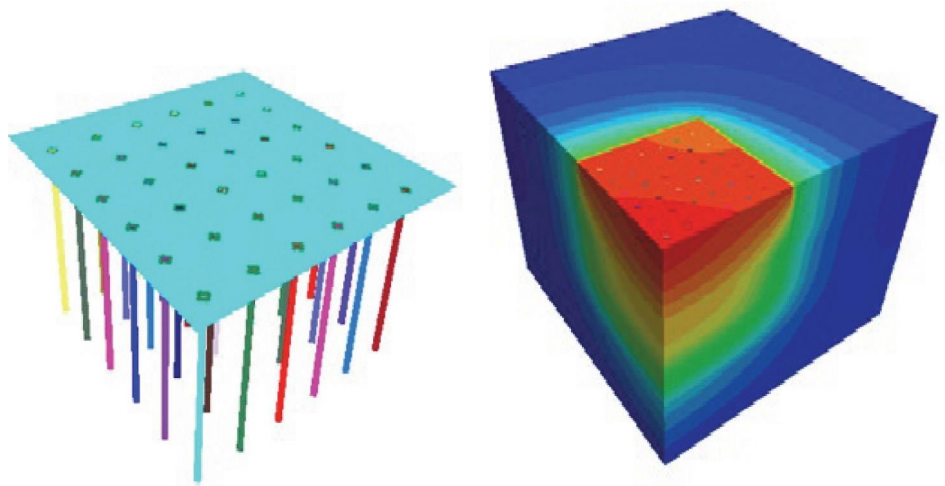

(a) (b)

Figure 4: (a) Model of piled raft and (b) overall boundary of the analysis.

represented by a distributed load on the surface of the raft. This lumped mass of the superstructure on the foundation method was previously us by Reul and Randolph [6], Sinha and Hanna [8], and others. In this numerical parametric study, the soil is modeled using the hexahedral element (brick) and pile and rafts are models using a structural element of pile and shell, respectively. The number of piles will vary hence depends on the available space on the raft. Due to the bisymmetric nature of the PRF (square) quarter of the foundation was taken to reduce very high-computational effort.

4.1. Unpiled Raft Foundation. The behavior of unpiled raft is taken as a reference for evaluating the performance of PRF in terms of the settlement and bearing capacity. The variation of settlement vs. step (the model analysis time) for uniform load is shown in Figure 7. The settlement profile is at the center, at some point and edge of the raft. The settlements at the center of the raft and edge are 196 and 104 mm. This results in a higher differential settlement of 92 mm. According to Boussinesq [35] the distribution of stress in an elastic medium by a point load decrease toward the edge resulting in a higher settlement at the center than at the edge.

The maximum positive bending moment is observed at the corners of the raft having a magnitude of 2. 25 MN m (Figure 8). The negative maximum bending moment is −1. 1 MN m located at the midsection of the raft in both x and y directions.

4.2. Influence of Pile Spacing. The center-to-center distance between two consecutive piles determines the number of the pile and the overall structural stiffness. Three different pile

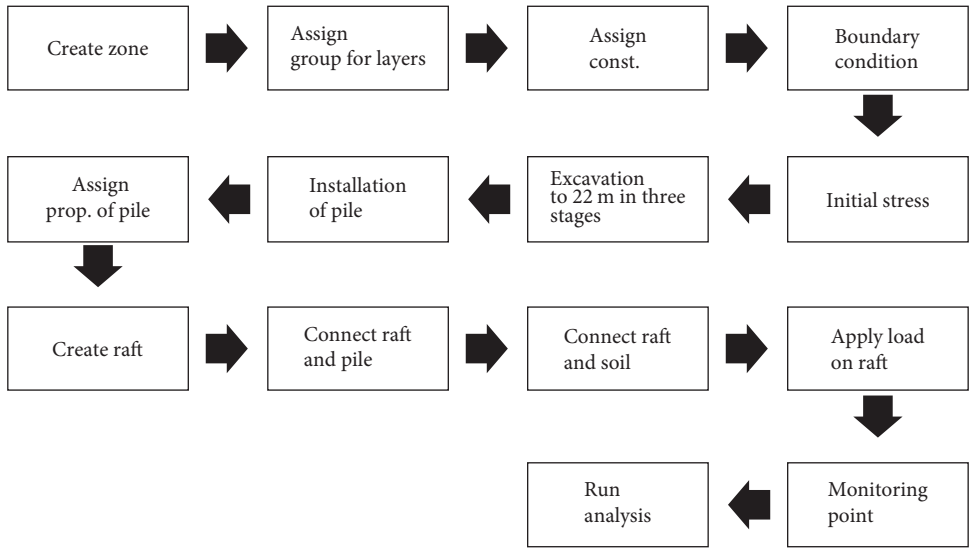

Figure 5: Static analysis procedure using FLAC3D.

Table 4: Summary of parametric values for numerical study of PRF.

Parameters	Unit	1st trial	2nd trial	3rd trial
Raft plane ($B \times L$)	m × m	39 × 39	39 × 39	39 × 39
Raft thickness	M	3	3	3
Pile length	M	10	15	20
Pile diameter	M	1	1.5	2
Pile spacing	M	3D	5D	7D

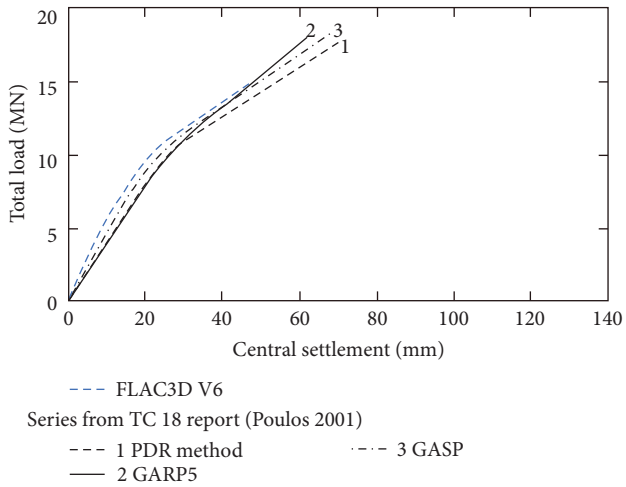

Figure 6: Settlement of piled raft for validation of software.

spacings (3D, 5D, and 7D) as a function of pile diameter are considered. Since most PRF systems in Addis Ababa have spacing of 3D and above. Table 5 depicts that increasing the spacing results in the increase of differential and total settlement. Especially at a spacing of 7D the differential and total settlement increases abruptly to 53 and 93 mm, respectively. This indicates that the pile spacing lower than 7D should be considered to alleviate settlement-related problems.

Where total settlement factor (ξs) is the ratio of the total settlement of un-PRF to PRF; differential settlement reduction factor ($\xi \Delta s$) is the ratio of the differential settlement of un-PRF to PRF; α_{pr} is the ration of the load taken by the pile to the raft. The reduction of load sharing is due to a decrease in the number of piles resulting in load to be shared by the raft. Load sharing of the raft has increased by 11.5% consecutively as the spacing increase. This result is close to the numerical result obtained from Reul and Randolph [6]. For all piles, the maximum bending moment and normalized lateral displacement were observed near the pile head, which decreased with an increase in the depth of the pile. The raft maximum and minimum bending moment are observed in the connection between pile–raft and corner of raft, respectively. A pile of 10-m length and 1-m diameter with different spacing consisting of three different spacings shows that increase of spacing results in to increase in bending moment of both pile and raft.

4.3. Influence of Pile Length. Pile length is a very crucial geometric component for skin friction piles. Hence the pile tip ends on hard rock, the majority of the loads transfer to soil largely through end bearing and in small fractions through skin friction. To capture the effect of pile length on the overall performance of PRF three different pile lengths (10, 15, and 20 m) are considered. The selected range of piles are commonly used in Addis Ababa specifically at Commercial Bank, Nib Bank, and other.

Due to modest increase in frictional resistance created by the pile skin, Figure 9 demonstrates that increasing pile length decreases overall settlement at varied rates. This reduction rate is very high for a pile diameter of 1 m due to smaller spacing between piles. The effectiveness of increasing pile length depends on the spacing between piles. Increasing pile length by 5 m from 10 m with a spacing of 3D reduces differential settlement is by 1 mm. Therefore, increasing pile length for the reduction of differential settlement is not significant.

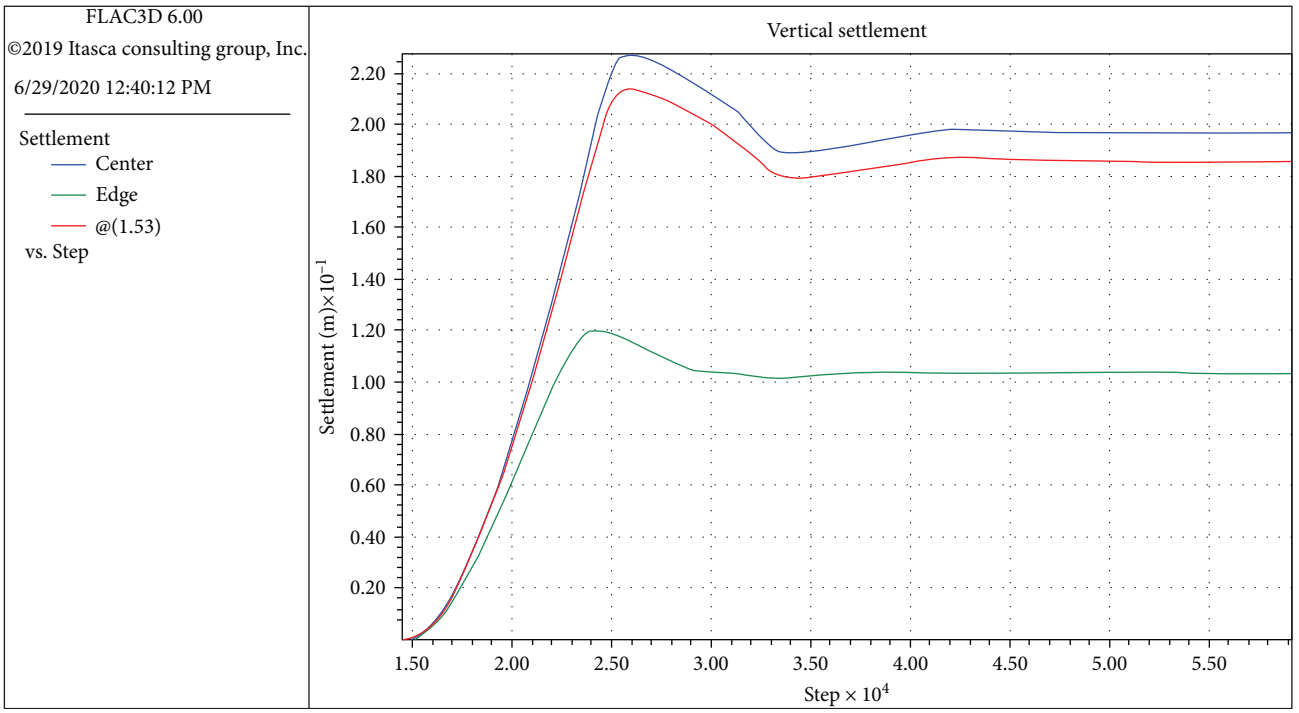

Figure 7: Settlement profile of unpiled raft.

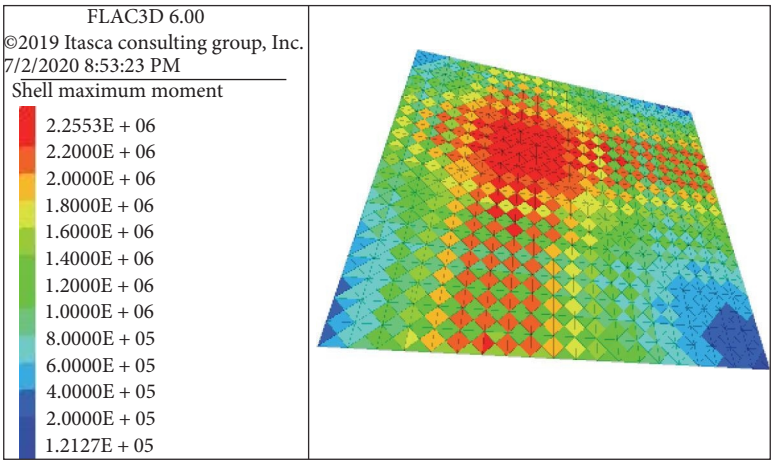

Figure 8: Maximum positive bending moment in unpiled raft foundation (MN.m).

Table 5: The results of the parametric study under different pile spacing.

Spacing	UPR	3D	5D	7D
No. of piles (–)	–	144	64	36
Length of pile (m)	–	10	10	10
Total settlement (mm)	196	69	57	93
Differential settlement	92	15	39	53
Ξs	–	0.35	0.29	0.47
$\xi\Delta$s	–	0.16	0.42	0.57
α_{pr}	–	0.76	0.67	0.53

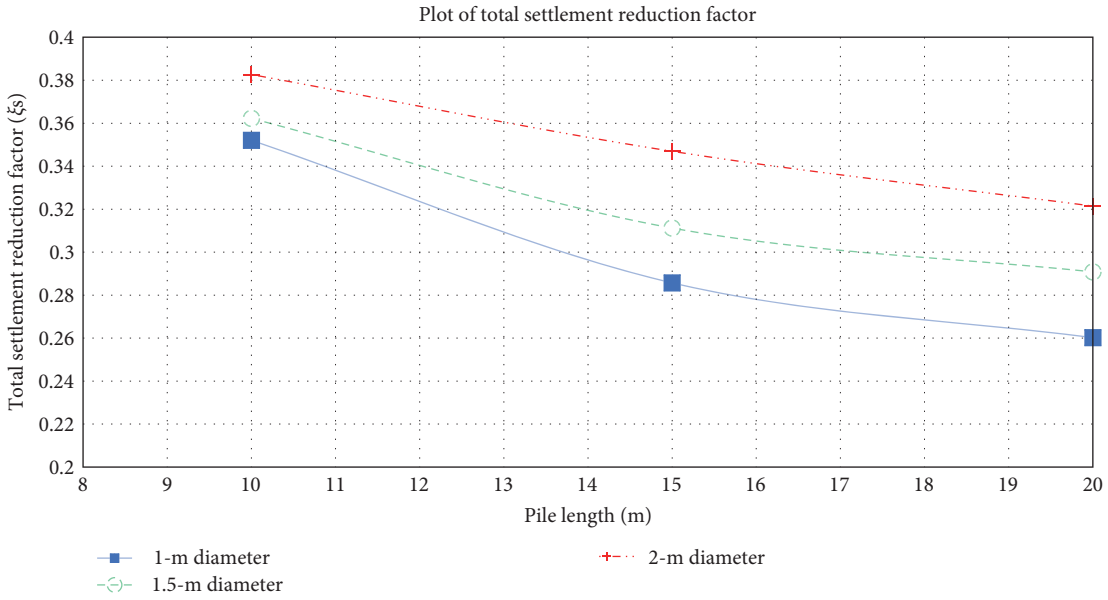

Figure 9: Total settlement reduction for different pile lengths and 3D spacing.

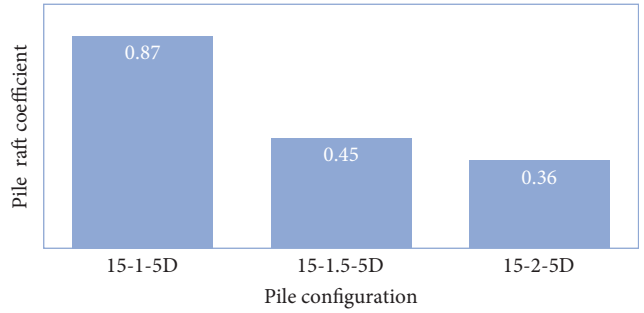

Figure 10: Piled raft coefficient for different pile diameter.

The load sharing behavior was also modified due to an increase in pile length. A pile of diameter 1.5 m, 5D (five times the pile diameter) spacing, and 10-m length share 37% of the total load, and the addition of pile length by 5 m increases the load sharing by 8%. Further increase of pile length by 10 m leads to increase of the load sharing by 6%. Hence, the pile raft coefficient increases when there is an increase in pile length with a relatively small percentage.

4.4. Influence of Pile Diameter. In this parameter, three different pile diameters (1, 1.5, and 2 m) are considered. A pile of 10-m length and 1-m diameter and nine number of piles has a total settlement of 93 mm. While the same number and length of the pile but a diameter of 2 m has a settlement of 63 mm. However, a pile of size 1.5 m and spacing of 5D has a higher settlement of 113 mm due to higher center-to-center spacing and long raft edge size. Figure 10 shows the variation of pile raft coefficient for a pile of 15-m length spaced at 5D. A diameter of 1 m has 64 total pile and piled raft coefficient of 0.87. Increase of pile diameter to 1.5 m reduces pile numbers to 36 and the coefficient to 0.45. This shows further increase of diameter leads in reduced pile raft coefficient to increase the load carried by the raft.

4.5. Influence of Raft Edge Dimension. The raft considered is a square of dimension 39×39 m and 3-m thick. The spacing between several piles determines the outer edge dimension of the raft. This intern influences differential and total settlement. As frequently observed from this numerical parametric study higher settlement is recorded either at the center or at the corner of the raft. A PRF having 20 m pile, 4.5 m spacing (1.5 diameter and 3D), and 0.75-m outer raft length has a corner settlement of 51 mm. However, the addition of the outer raft dimension by 3 m increases the raft corner settlement by 13 mm. The general settlement trend is dependent on the center-to-center spacing of pile and raft edge dimensions.

4.6. Optimized Design of PRF. The foundation design depends on the geologic condition, load type and magnitude, foundation type, and intended purpose. The optimized design is providing a small total pile length with an acceptable limit of design requirement. In the previous parametric study, it has been found that the main parameters that control total, differential settlement, and load sharing of PRF are the pile spacing and raft edge dimension from the pile periphery. Hence, to achieve an optimized design a new

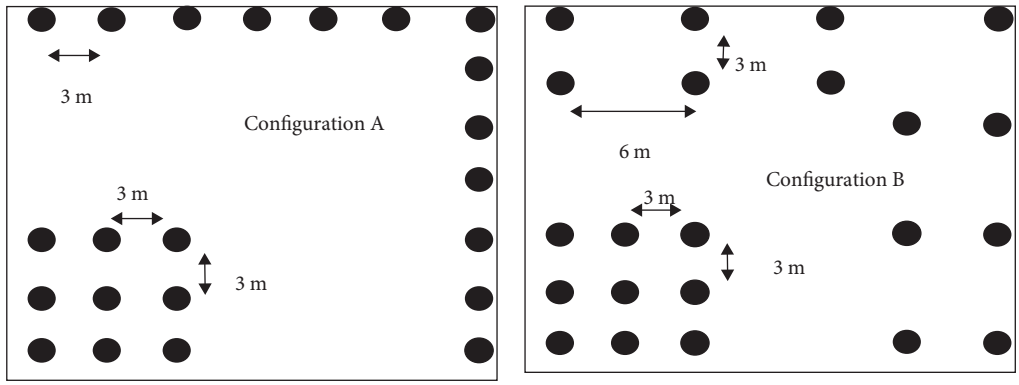

Figure 11: Modified pile configurations (a) pile at the center and edge and (b) pile at the center and two rounds of edge.

Table 6: Results of optimized piles raft configuration.

Parameters	Uniform pile	Configuration A	Configuration B
No. of piles (–)	144	88	84
Total pile length (m)	1,440	880	840
Apr	0.76	0.53	0.49
ξs	0.35	0.4	0.4
$\xi \Delta s$	0.16	0.32	0.04

pile configuration, piles are placed under the center of the edge of the raft is proposed (Figure 11) and its performance was be evaluated (Table 6).

The modified pile configuration B (Figure 11(b)) has achieved a maximum economy by saving 41% of the piles used. In this configuration differential settlement was only 4 mm (has reduced 95% differential settlement) due to the addition of the second round of piles around the raft edge. In addition, Table 6 shows the modified pile raft configuration B transfer 50% of the superstructural load to the raft and the rest to the pile which is usually appreciated.

5. Conclusion

Based on the study, the following conclusions are drawn:

(i) Generally, pile length and diameter have little use in reducing settlement. However, the fundamental factors that affect settlements are pile spacing the extended distance of a raft from the outermost pile. The raft settles at the center more than any other portion of the PRF in the shape of a bowl. The differential settlement is governed by the extended distance of raft from the outermost pile periphery. Hence, pile diameter should be balanced with raft edge dimension to control differentials settlement.

(ii) Spacing has a considerable effect in raising the load shared by the raft. Extending pile length has reduced the load shared by the raft. The total settlement increases from 57 to 93 mm for spacing increases from 5D to 7D mm. Load sharing of the raft has increased by 11.5% consecutively as the spacing increase from 3D to 7D. Despite variations in pile length and diameter and controlled settlement, a close load sharing between the pile and raft is accomplished at a separation of seven times the pile diameter.

(iii) The installation of piles results in increases in the negative bending moment of the raft compared with an unpiled raft due to variability of stiffness in underneath soil and pile. Generally, bending moment in the raft increases as the spacing and pile diameter increase. The piles bending moment has shown an increase with the length and diameter of the piles due to high-slenderness ratio.

(iv) An optimized design of PRF depends mainly on the pile center-to-center spacing and raft outer edge dimension from the periphery of the pile. Optimized design of piled raft is attained by placing piles at the center and edge of the raft. While pile length and diameter variation have no significant influence on optimized design. Optimized piled raft configuration B (piles covering an area at the center $A_G/A_R = 0.25$ or quarter of the raft area is covered by piles and two rounds of pile around the edge of the raft) proposed has reduced the number of piles by 41% and differential settlement by 95%.

6. Limitation and Future Prospective

This study is conducted on one specific case study which is commercial bank headquarter skyscraper. Experimental study and comparison with the numerical method are

beyond the scope of this study that may be addressed for the future works.

Data Availability

The data used to support the study are available from the corresponding author upon request (argaw.asha@astu.edu.et) or (getmaree888@gmail.com).

Disclosure

A preprint has previously been published in Adama Science and Technology University of Thesis Work [36].

Conflicts of Interest

The authors declare that they have no conflicts of interest.

Acknowledgments

The Adama Science and Technology University funded the work presented in the research as part of thesis work.

References

[1] H. G. Poulos, *Methods of Analysis of Piled Raft Foundations: A Report Prepared on Behalf of Technical Committee TC18 of Piled Foundations*, International Society of Soil Mechanics and Geotechnical Engineering, London, 2001.

[2] R. Katzenbach, A. Schmitt, and J. Turek, "Assessing settlement of high-rise structures by 3D simulations," *Computer-Aided Civil and Infrastructure Engineering*, vol. 20, no. 3, pp. 221–229, 2005.

[3] A. Mandolini, R. Di Laora, and Y. Mascarucci, "Rational design of piled raft," *Procedia Engineering*, vol. 57, pp. 45–52, 2013.

[4] H. G. Poulos and G. Bunce, "Foundation design for the Burj Dubai—the world's tallest building," in *International Conference on Case Histories in Geotechnical Engineering*, 2008.

[5] H. G. Poulos, "Simplified design," in *Deep Foundations 2002*, vol. 256 of *32*, pp. 441–458, American Society of Civil Engineers, Virginia, US, 2002.

[6] O. Reul and M. F. Randolph, "Design strategies for piled rafts subjected to nonuniform vertical loading," *Journal of Geotechnical and Geoenvironmental Engineering*, vol. 130, no. 1, pp. 1–13, 2003.

[7] M. F. Randolph, "Design methods for pile groups and piled rafts," in *13th International Conference on Soil Mechanics and Foundation Engineering*, pp. 61–82, International Journal of Geoengineering Case Histories (ISSMGE), New Delhi, 1994.

[8] A. Sinha and A. M. Hanna, "3D Numerical model for piled raft foundation," *International Journal of Geomechanics*, vol. 17, no. 2, Article ID 04016055, 2017.

[9] B. Sheil, "Numerical simulations of the reuse of piled raft foundations," *Acta Geotechnica*, vol. 12, pp. 1047–1059, 2017.

[10] H. C. Bernardes, H. L. de Souza Filho, A. D. Dias, and R. P. da Cunha, "Numerical analysis of piled raft foundations designed for settlement control on steel grain silos in collapsible soils," *International Journal of Civil Engineering*, vol. 19, no. 5, pp. 607–622, 2021.

[11] K. Fisseha, *Investigating the load sharing behaviour of piled raft with pile tips on hard strata using finite element method: case of Commercial Bank of Ethiopia headquarters building*, Masters Thesis, Addis Ababa University, 2019.

[12] A. M. J. Alhassani and A. N. Aljorany, "Parametric study on unconnected piled raft foundation using numerical modelling," *Journal of Engineering*, vol. 26, no. 5, pp. 156–171, 2020.

[13] P. Deb and S. K. Pal, "Structural and geotechnical aspects of piled raft foundation through numerical analysis," *Marine Georesources & Geotechnology*, vol. 40, no. 7, pp. 823–846, 2022.

[14] D. A. Mangnejo, M. A. Soomro, N. Mangi, I. A. Halepoto, and I. A. Dahri, "A parametric study of effect on single pile integrity due to an adjacent excavation induced stress release in soft clay," *Engineering, Technology & Applied Science Research*, vol. 8, no. 4, pp. 3189–3193, 2018.

[15] M. Y. Fattah, M. J. Al-Mosawi, and A. A. O. Al-Zayadi, "Time dependent behavior of piled raft foundation in clayey soil," *Geomechanics and Engineering*, vol. 5, no. 1, pp. 17–36, 2013.

[16] P. Deb and S. K. Pal, "Analysis of load distribution coefficient of piled raft system: a numerical approach," in *Foundation and Forensic Geotechnical Engineering, IGC 2021*, K. Muthukkumaran, C. N. V. S. Reddy, A. Joseph, and S. Senthamilkumar, Eds., Lecture Notes in Civil Engineering, pp. 129–137, Springer, Singapore, 2021.

[17] Y. F. Mohammed, A. A.-O. Moataz, and A. A. Fouad, "Effect of number of piles on load sharing in piled raft foundation system in saturated gypseous soil," *International Journal of Civil Engineering and Technology*, vol. 9, no. 3, pp. 932–944, 2018.

[18] P. Deb, B. Debnath, R. B. Reang, and S. K. Pal, "Structural analysis of piled raft foundation in soft soil: an experimental simulation and parametric study with numerical method," *Ocean Engineering*, vol. 261, Article ID 112139, 2022.

[19] M. Y. Fattah, M. A. Yousif, and S. M. K. Al-Tameemi, "Effect of pile group geometry on bearing capacity of piled raft foundations," *Structural Engineering and Mechanics*, vol. 54, no. 5, pp. 829–853, 2015.

[20] D. Hadi, M. Waheed, and M. Fattah, "Effect of pile's number on the behavior of piled raft foundation," *Engineering and Technology Journal*, vol. 39, no. 7, pp. 1080–1091, 2021.

[21] H. Moayedi, R. Nazir, S. Ghareh, A. Sobhanmanesh, and Y.-C. Tan, "Performance analysis of a piled raft foundation system of varying pile lengths in controlling angular distortion," *Soil Mechanics and Foundation Engineering*, vol. 55, no. 4, pp. 265–269, 2018.

[22] J. Ko, J. Cho, and S. Jeong, "Nonlinear 3D interactive analysis of superstructure and piled raft foundation," *Engineering Structures*, vol. 143, pp. 204–218, 2017.

[23] L. Gu, Z. Wang, Q. Huang, G. Ye, and F. Zhang, "Numerical investigation into ground treatment to mitigate the permanent train-induced deformation of pile-raft-soft soil system," *Transportation Geotechnics*, vol. 24, Article ID 100368, 2020.

[24] P. V. Lade, "Overview of constitutive models for soils," in *Soil Constitutive Models*, pp. 1–46, American Society of Civil Engineers, Virginia, 2005.

[25] E. B. C., *7. Standar, Foundations*, Ministry of Work and Urban Development, Addis Ababa, 1995.

[26] Itasca, *Fast Lagrangian Analysis of Continua in 3-Dimension (FLAC3D V 5.01)*, Itasca Consulting Group, Minneapolis, MN, USA, 2012.

[27] K. S. Ti, B. B. Huat, J. Noorzaei, M. S. Jaafar, and G. S. Sew, "A review of basic soil constitutive models for geotechnical application," *Electronic Journal of Geotechnical Engineering*, vol. 14, pp. 1–18, 2009.

[28] J. T. Chavda and G. R. Dodagoudar, "Finite element evaluation of ultimate capacity of strip footing: assessment

using various constitutive models and sensitivity analysis," *Innovative Infrastructure Solutions*, vol. 3, no. 1, 2018.

[29] K. Yamashita, M. Tomono, and M. Kakurai, "A method for estimating immediate settlement of piles and pile groups," *Soils and Foundations*, vol. 27, no. 1, pp. 61–76, 1987.

[30] R. E. Goodman and F. H. Kulhawy, "Design of foundations on discontinuous rock," in *International Conference on Structural Foundations on Rock*, pp. 209–220, TRID, Sydney, Australia, 1980.

[31] G. Feo, "Foundation design and costruction-Publication No. 1," 2006.

[32] J.-L. Briaud, *Geotechnical Engineering: Unsaturated and Saturated Soils*, Wiley, Hoboken, 2013.

[33] D. G. Lin, W. T. Liu, and J. C. Chou, "Load transfer and deformation analyses of piled-raft foundation in taipei metropolitan," *Journal of Marine Science and Technology*, vol. 24, no. 4, pp. 798–806, 2016.

[34] T. L. Orr and E. R. Farrell, *Geotechnical Design to Eurocode 7*, Springer Science & Business Media, 2012.

[35] V. J. Boussinesq, *Application des potentiels a l'étude de l'e quilibre et du movement des solides élastiques*, Gauthier-Villars, Imprimeur-Libraire, Paris, 1885.

[36] G. M. Yirsaw, *Numerical study of piled raft foundation under vertical static and seismic loads*, Unpublished Master's Thesis, Adama Science and Technology University, 2020.